JOURNAL OF MATERIALS SCIENCE **37** (2002) 765–779

Self-consistent forms of the chemical rate theory of Ostwald ripening

R. N. STEVENS, C. K. L DAVIES
Department of Materials, Queen Mary, University of London, London E1 4NS, UK

The chemical rate theory of Ostwald ripening introduced by A. D. Brailsford and P. Wynblatt (*Act. Metall.* **27** (1979) 498) determines the mean growth rate of particles of a particular size class by solving the diffusion equations for a representative particle (radius r) surrounded by a shell of matrix (the averaging sphere, radius r_A) outside which there is a homogeneous effective medium averaging the emission and absorption of solute atoms by the remainder of the particles. Brailsford and Wynblatt set $r = r_A$, in effect removing the matrix shell. It is argued herein that the feature of the theory so omitted is a very important one and we therefore use it to develop and extend the theory to make it self-consistent in the sense that the mean ratio of the particle and averaging sphere volumes is equal to the volume fraction of particles. Three self-consistent versions are developed, two of which have r_A relatively constant for small particles and slowly increasing for particles greater than approximately average size. These were motivated by the observation from numerical simulations that small particles are little influenced by their neighbours whereas larger particles are much more strongly affected by the environment. Analytical expressions in terms of experimentally observable variables are given for the probability distributions for particle sizes, and tables of the parameters required to evaluate the distribution functions as a function of volume fraction are provided. It is concluded that the properties of the Brailsford and Wynblatt effective medium are closely reproduced by the alternative analytical theories, but that the idea of a matrix shell round the representative particle is unique to the chemical rate theory. It is argued that this feature makes the theory flexible and adaptable. This adaptability could be used to reproduce the results of sophisticated numerical simulations in a form which would be computationally efficient to include in wider simulations involving, say, the effect of particle growth on long term mechanical properties.

1. Introduction

In systems with microstructures consisting of a dispersion of small particles embedded in a continuous matrix there is thermodynamic motivation for competitive growth of the particles since this will result in a reduction in interfacial area and hence in total free energy. In the late stages of phase separation when the volume fraction of the embedded phase is nearly constant, the process is usually termed particle coarsening or Ostwald ripening [1]. The theory of Ostwald ripening was first put on a sound footing by Liftshitz and Slyozov [2] and independently by Wagner [3] (the LSW theory) after earlier work by Greenwood [4]. In the limit of long ageing times the theory shows that the (time independent) probability density, $p(\rho)$ (where $p\,\mathrm{d}\rho$ is the probability of a particle having a relative size between $\rho = r/\langle r\rangle$ and $\rho + \mathrm{d}\rho$) is

$$p = \frac{4\rho^2 \exp\left[\dfrac{-\rho}{3/2-\rho}\right]}{9(1-2\rho/3)^{11/3}(1+\rho/3)^{7/3}}, \qquad (1)$$

where r is the particle radius and angled brackets indicate mean or average value. The theory also provides an expression for the growth rate of the average size, $\langle r\rangle$,

$$\langle r\rangle^3 - \langle r_0\rangle^3 = kt. \qquad (2)$$

where $\langle r_0\rangle$ is the average particle size at time $t = 0$, and k, is a combination of physical constants. Equations of this form provide all the information necessary to determine the actual particle sizes and inter-particle spacings as a function of time.

However, the theory assumes that particles are so far apart that the diffusion field of any particle and hence its growth rate depends only on its size and not on the environment provided by its neighbours. It is therefore a theory applicable to the limiting case of zero volume fraction. In a system with a finite volume fraction of the embedded phase, particles of the same size will have different environments and thus different diffusion fields and growth rates. In order to use the LSW method to solve the problem, the *mean* growth rate of particles of a given size class is required as a function of size. Mean field theories [5–11] hope to choose the diffusion field in such a way as to produce the correct mean growth rate while other theories use formal solutions to

the multi-particle diffusion problem to determine expressions for the mean growth rate for a particular size class using various techniques [12–17]. Mean growth rate and mean field theories are two sides of the same coin since a mean field always implies a mean growth rate and a mean growth rate a mean field. Another general class of methods for the study of the problem is provided by numerical simulation [8, 17–22]. A very different approach was outlined by Liftshitz and Slyozov themselves and developed later by Davies *et al.* [23]. While reviews covering some or all of these methods have been provided by Jayanth and Nash [24], Voorhees [25, 26] and Mullins and Viñals [27] no detailed analytical comparison between the theories has been made.

The chemical rate theory of Ostwald ripening, due to Brailsford and Wynblatt [5], is a mean field theory based on an "effective medium", a homogeneous medium averaging the emission and absorption of solute in the environment of the particle whose growth rate is being sought. The solution of the diffusion equation for a particle representative of a particular size class embedded in the effective medium gives the mean growth rate for that size. The theory has been little used and has received little development since it was introduced. The present work aims to further develop the theory and to put it in a form making its results easily accessible for comparison with experiment. There is one particular feature of the theory which is unused in spite of the fact that the physical basis for it seems clear. This feature is identified in Sections 2 and 3 below and another of the aims here is to develop the potential of the theory as fully as possible. It is also noted that, in mean growth rate and mean field theories, analytical expressions are usually given for the probability distribution and for the growth rate of the mean size but the parameters in these are not explicitly given in terms of volume fraction. A computer program is usually necessary to evaluate the parameters, and consequently those involved in experiments in coarsening do not find it easy to compare their experimental results with the various theoretical predictions. As noted above, an important aim here is to produce results in a form readily accessible to those doing experiments. The relationship of the chemical rate theory with other theories will also be made clear.

2. Chemical rate theory

Both mean growth rate theories and mean field theories lead to an expression for the average growth rate, $\dot{r} = \mathrm{d}r/\mathrm{d}t$, which can be written in the form

$$\dot{r} = K\frac{1}{r}\left(\frac{1}{r^*} - \frac{1}{r}\right)W, \tag{3}$$

where t is time, K is another combination of physical constants which equals $9k/4$ in the zero volume fraction case, r^* is the size of a particle which neither grows nor shrinks and W is a dimensionless (scaling invariant) parameter, in general a function of volume fraction, ϕ, r and t which can be regarded as the ratio of the growth rate at a volume fraction ϕ and the zero volume fraction growth rate. The determination of W therefore solves the problem of the effect of volume fraction on particle coarsening. The diffusion equations obey the superposition principle and this implies that W should approach 1 as r approaches zero.

The function W is involved in a number of useful relations. The sink strength, B, [18, 25] is a dimensionless quantity proportional to $r^2\dot{r}$ and thus to the rate of emission or absorption of solute by a particle of size r. Using Voorhees' definition of B [25] we have, from Equation 3

$$B = \frac{1}{K}r^2\dot{r} = \left(\frac{r}{r^*} - 1\right)W = (y-1)W, \tag{4}$$

where $y = r/r^*$. This relates W and B.

The average value of B, is also proportional to the rate of change, during coarsening, of volume fraction, $\mathrm{d}\phi/\mathrm{d}t$, which becomes asymptotically zero at long times. Applying this to Equation 3 or 4 gives

$$r^* = \frac{\int_0^\infty rWf(r,t)\,\mathrm{d}r}{\int_0^\infty Wf(r,t)\,\mathrm{d}r}, \tag{5}$$

(where $f\,\mathrm{d}r$ is the number of particles per volume with size between r and $r + \mathrm{d}r$) or

$$\langle W\rangle = \langle yW\rangle, \tag{6}$$

showing that r^* is a weighted mean of r with W as the weight factor.

The effective medium in the chemical rate theory is a homogeneous continuum in which there is, at every point, a rate at which solute is created and a rate at which solute is absorbed. Corresponding to particles with radii between r and $r + \mathrm{d}r$ there is an emission rate $P(r,t)\,\mathrm{d}r$ (moles per second per mole of system) and a sink rate $Dk^2(r,t)c_\infty\,\mathrm{d}r$ with the same units where D is the diffusivity, c_∞ the average mole fraction of solute in the matrix and k^2 a parameter called the sink factor density. The total emission rate, $P_\mathrm{T}(t)$ and the total sink factor, $k_\mathrm{T}^2(t)$ are found by integrating $P\,\mathrm{d}r$ and $k^2\,\mathrm{d}r$ over all particle sizes.

The model for solving the diffusion equation is illustrated in Fig. 1. The system is divided into three regions, the particle itself, of radius r, a spherical shell of matrix (the averaging sphere) of outer radius r_A, and the surrounding homogeneous medium. As will be seen, this spherical shell of matrix is the unused feature of the theory. The flux is assumed to be radial and that steady state conditions prevail. The flux is divergence-less in the region between r and r_A, and has a divergence equal and opposite to the net total emission/absorption rate in the homogeneous medium ($r > r_\mathrm{A}$). At $r = r_\mathrm{A}$, there is no discontinuity in either the solute concentration or its gradient. At infinite distance from the particle c approaches c_∞ while at the particle surface it is $c\,(r)$ determined by setting the flux, J_I, of solute across the particle/matrix interface equal to the diffusion flux in the matrix at the particle surface. If c_r is the solute concentration in equilibrium with the particle of size r given by

$$c_r = c_\mathrm{e}\left(1 + \frac{l}{r}\right), \tag{7}$$

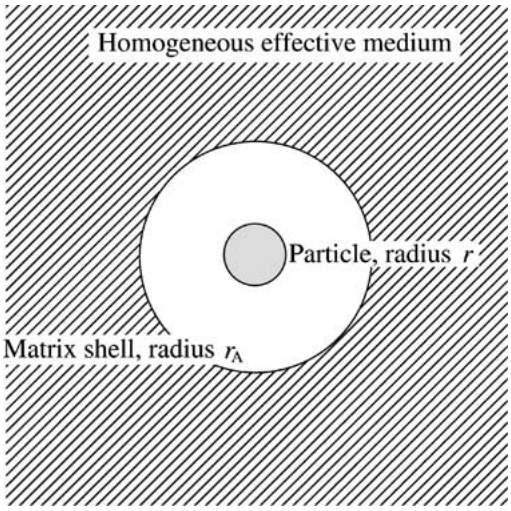

Figure 1 Model for the solution of the diffusion equation to find the average growth rate of particles in the size class r to $r + \mathrm{d}r$.

where l is the capillarity length, then

$$J_I = v_I[c(r) - c_r]/V_m, \tag{8}$$

where v_I is a parameter called the solute transfer velocity and V_m is the molar volume.

With these boundary conditions the solution given by Brailsford and Wynblatt [5] yields,

$$W(r, r_A, t) = \frac{v_I r(1 + k_T r_A)}{D(1 + k_T r) + v_I r[1 + k_T(r_A - r)]}, \tag{9}$$

and

$$k_T^2 = \int_0^\infty 4\pi r W(r, r_A, t) f(r, t)\,\mathrm{d}r. \tag{10}$$

Following Lifshitz and Slyozov [2] the equations are solved by first making a mathematical transformation to dimensionless variables, replacing r by y and t by τ where

$$y = r/r^* \tag{11}$$

and

$$\tau = \ln(r^*/r_0^*), \tag{12}$$

where r_0^* is the critical size when the reduced time, $\tau = 0$. The dimensionless sink factor, q, and the dimensionless averaging sphere radius, Y, are defined by

$$q = k_T r^*, \tag{13}$$

and

$$Y = r_A/r^*, \tag{14}$$

which allows us to write $W(r, r_A, t)$ in the form

$$W(y, \phi, \tau) = \frac{\omega y(1 + qY)}{e^{-\tau}(1 + qY) + \omega y[1 + q(Y - y)]}, \tag{15}$$

where the parameter ω determines the relative importance of the rates of matrix diffusion and transfer of solute across the interface and is given by

$$\omega = v_I r_0^*/D. \tag{16}$$

With these definitions Equation 3 becomes

$$U = \frac{\mathrm{d}y}{\mathrm{d}\tau} = \frac{\gamma(\phi, \tau)W(y, \phi, \tau)(y - 1)}{y^2} - y, \tag{17}$$

where the parameter $\gamma(\phi, \tau)$ is given by

$$\gamma(\phi, \tau) = \frac{K}{r^{*2}}\frac{\mathrm{d}t}{\mathrm{d}r^*}. \tag{18}$$

The number of particles per volume with y between y and $y + \mathrm{d}y$ is $\psi(y, \tau)\,\mathrm{d}y$ (where $\psi = r^* f(r, t)$) with the distribution function, ψ, subject to the continuity equation,

$$\frac{\partial \psi}{\partial \tau} + \frac{\partial}{\partial y}(U\psi) = 0. \tag{19}$$

Using the new variables together with the expression for volume fraction in terms of n, the total number of particles per volume and r^{*3} , (i.e. $\phi = 4\pi r^{*3}\langle y^3\rangle n/3$), Equation 10 gives

$$q^2 = \frac{3\langle yW\rangle\phi}{\langle y^3\rangle} = \frac{3\langle W\rangle\phi}{\langle y^3\rangle}, \tag{20}$$

where Equation 6 has been used to obtain the second expression.

At large τ, ϕ becomes asymptotically constant and the term $e^{-\tau}(1 + qY)$ in the expression for W, Equation 15, approaches zero. The factor W then becomes

$$W = \frac{1 + qY}{1 + q(Y - y)}. \tag{21}$$

Lifshitz and Slyozov [2] and Brailsford and Wynblatt [5] show in these circumstances that solute conservation requires that $\gamma(\phi, \tau)W(y, \phi, \tau)$ becomes time independent (which effectively means that γ, W and hence q all become time independent) and that U has a double root at $y = y_c$. Particles of sizes greater than y_c do not exist in the distribution. It also becomes possible to factorise ψ into the product of a term equal to the number of particles per volume, $n(\tau)$, depending only on time and a probability density, $p'(y)$, depending only on particle size, and the solution to Equation 19 gives

$$p'(y) = \frac{C}{|U(y)|}\exp\left[3\int_0^y \frac{\mathrm{d}y'}{U(y')}\right]. \tag{22}$$

It can be shown using the method of Lifshitz and Slyozov [2] that the distribution, p', is normalized if the constant $C = 3$ independent of volume fraction. In order to find p' together with y_c and γ and thus solve the problem, we need to establish the relationship between Y and y so that Equation 22 can be integrated.

3. Specific asymptotic solutions

The forms of the $Y(y)$ function which have been used or proposed are illustrated in Fig. 2. Brailsford and Wynblatt [5] used the simplest possible form, $Y = y$. This sets the thickness of the matrix shell at zero and therefore does not use this feature of the theory. It is noted that the one region in the system in which it is inappropriate to smear out the particles into a continuum is in the vicinity of the representative particle whose growth rate is being sought. The heterogeneous

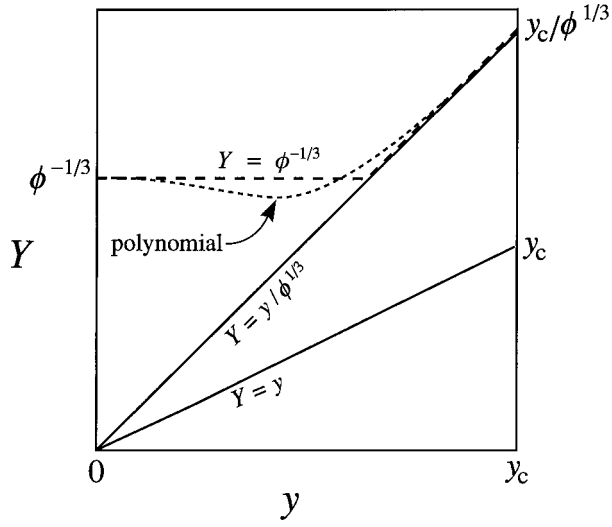

Figure 2 Forms of the $Y(y)$ function used to find the W function. For convenience, the curves have been drawn with the same value of cut-off size, y_c, but if used to solve the problem for a given volume fraction, ϕ, each would generate a different value of y_c.

nature of the real system cannot easily be ignored in this region. Brailsford and Wynblatt, recognising this, did point out that the form $Y = y$ was not consistent with the model [5]. The effective medium averages the emission and absorption of solute by the particles surrounding the representative particle, replacing them with a homogeneous continuum with properties depending on volume fraction. The identity of the representative particle is retained, however, and it is surrounded by a shell of matrix. If the immediate environment of the representative particle is to be consistent with the properties of the effective medium, the ratio of particle volume and the averaging sphere volume should be equal to the volume fraction. They therefore proposed (but did not implement) the self-consistent form $Y = y/\phi^{1/3}$ which satisfies this condition for every particle.

It seems intuitively obvious, however, that smaller particles are much less influenced by their environment than are larger particles. They are shrinking much faster than any nearby super-critical particles are growing, and are much further from all their neighbours in terms of their own radii than are large particles. The environment is represented by the effective medium, and its influence on small particles would be reduced if it were further away from them (i.e. Y were relatively larger) than for large particles. On the basis of numerical simulations Voorhees [10, 25, 22] suggested that a more realistic form for the averaging sphere radius would be $Y = \phi^{-1/3}$ for $0 < y \leq 1$ and $Y = y/\phi^{1/3}$ for $1 < y \leq y_c$. This is also shown in Fig. 2. The proposal is not self-consistent in the sense that Brailsford and Wynblatt use the term. However, the idea that the local environment of the representative particle must be consistent with the properties of the effective medium can be retained in an average sense. So, while the average of the ratio of particle volume to averaging sphere volume for all particles must be equal to ϕ, small particles can have a smaller value for the ratio and large particles a larger value, taking into account the differing impact of the environment on their growth rates. If the *average* of the ratio of particle volume to averaging sphere volume for all particles is ϕ_a, then the overall condition for self-consistency is $\phi_a = \phi$. There is an infinite number of ways in which this can be achieved, but a self-consistent model similar to Voorhees' suggestion might be found by using a line of slope *lower* than $\phi^{-1/3}$ for Y in the range $1 < y \leq y_c$. The contributions to the average lower than ϕ from particles with $0 < y \leq 1$ would be off-set by contributions higher than ϕ from particles with $1 < y \leq y_c$ and if the slope were chosen correctly, ϕ_a, the average ratio of particle and averaging sphere volumes, could be made equal to ϕ.

Results of this kind are reported herein but polynomials have been used to represent $Y(y)$ because of the awkwardness caused by the discontinuity of slope in Voorhees' original suggestion. A polynomial model is illustrated schematically in Fig. 2. The intention is to make this model self-consistent, in a way which is analogous to that described above for the Voorhees' suggestion, by varying one of the parameters describing the polynomial, but solutions for arbitrary values of the parameters have to be found first since the distribution functions are required to find the apparent volume fractions. We have three models for $Y(y)$: (1) the Brailsford and Wynblatt proposal, $Y = y/\phi^{1/3}$ which is inherently self-consistent, (2) $Y(y)$ represented by a quadratic polynomial and (3) $Y(y)$ represented by a cubic polynomial; the latter two will be made self-consistent by a procedure which will be described subsequently. Model 1 is a special case of model 2 hence we begin with 2.

3.1. Model 2—$Y(y)$ represented by a quadratic

The quadratic has an intercept at $y = 0$ of $\zeta/\phi^{1/3}$ and a value and slope at $y = y_c$ of $\mu y_c/\phi^{1/3}$ and $\mu/\phi^{1/3}$ respectively. With the parameters $\zeta = \mu = 1$ we have a quadratic representation of Voorhees' suggestion and one or both of the parameters can be varied to obtain self-consistency. The quadratic is given by

$$Y = \phi^{-1/3}\left[\zeta + y(\mu - 2\zeta/y_c) + y^2\zeta/y_c^2\right], \qquad (23)$$

where the parameters ζ and μ are such that $0 \leq \zeta \leq 1$ and $\phi^{1/3} \leq \mu \leq 1$ with y_c the upper cut-off value of y. An explicit expression for W can now be given using Equations 21 and 23,

$$W = \frac{\lambda_0 + (\lambda_1 + q)y + \lambda_2 y^2}{\lambda_0 + \lambda_1 y + \lambda_2 y^2}, \qquad (24)$$

where

$$\left.\begin{aligned} \lambda_0 &= 1 + \zeta\alpha/\mu \\ \lambda_1 &= \alpha[1 - 2\zeta/(\mu y_c)] - q \\ \lambda_2 &= \alpha\zeta/\left(\mu y_c^2\right) \end{aligned}\right\}, \qquad (25)$$

with

$$\alpha = \mu q/\phi^{1/3}. \qquad (26)$$

The expression for U, the growth rate, is, using Equations 17 and 24,

$$U = \frac{-\lambda_2 y^5 - \lambda_1 y^4 + (\gamma\lambda_2 - \lambda_0)y^3 + \gamma[\lambda_1 + q - \lambda_2]y^2 + \gamma[\lambda_0 - (\lambda_1 + q)]y - \gamma\lambda_0}{y^2\left(\lambda_0 + \lambda_1 y + \lambda_2 y^2\right)} \tag{27}$$

and putting $U = 0$ at $y = y_c$ we find a relationship between γ and y_c:

$$\gamma = \frac{y_c^3(1 + \beta y_c)}{(y_c - 1)(1 + \alpha y_c)}, \tag{28}$$

where

$$\beta = \alpha - q. \tag{29}$$

Applying the condition that both U and dU/dy are zero at $y = y_c$ yields an expression from which γ can be eliminated to give an expression for y_c alone:

$$-2\alpha\beta y_c^3 + (3\alpha\beta - 3\beta - \alpha)y_c^2 + (4\beta + 2\alpha - 2)y_c + 3 = 0, \tag{30}$$

the positive root of which is y_c.

To evaluate the integral in Equation 22 we have to factorise the polynomial, P_5, in the numerator of Equation 27. Knowing y_c from Equation 30, we can deflate P_5 by $(y - y_c)^2$ to obtain a cubic, P_3. The form of the integral in Equation 22 depends on how many real roots P_3 has. There are two possible forms, each applicable in different ranges of ζ and μ:

$$I = \int_0^y \frac{y'^2(\lambda_0 + \lambda_1 y' + \lambda_2 y'^2)}{-\lambda_2(y_c - y')^2(y' + y_1)(y' + y_2)(y' + y_3)}\,dy' \tag{31}$$

and

$$I = \int_0^y \frac{y'^2(\lambda_0 + \lambda_1 y' + \lambda_2 y'^2)}{-\lambda_2(y_c - y')^2(y' + y_1)(y'^2 + v'y' + w')}\,dy' \tag{32}$$

where $-y_1$, $-y_2$ and $-y_3$ are real roots of P_3, or $-y_1$ a real root with v' and w' the coefficients of the quadratic factor when there are two complex roots.

Integration of Equations 31 and 32 allows an expression for p' to be found using Equation 22. The results are

$$p' = \frac{3y^2\left(\lambda_0 + \lambda_1 y + \lambda_2 y^2\right)\exp\left(\dfrac{-cy}{y_c - y}\right)}{\gamma\lambda_0(1 - y/y_c)^a(1 + y/y_1)^{b_1}(1 + y/y_2)^{b_2}(1 + y/y_3)^{b_3}} \tag{33}$$

and

$$p' = \frac{3y^2(\lambda_0 + \lambda_1 y + \lambda_2 y^2)\exp\left(\dfrac{-cy}{y_c - y}\right)\exp\left[M\tan^{-1}\left(\dfrac{y\sqrt{w' - v'^2/4}}{w' - v'y/2}\right)\right]}{\gamma\lambda_0(1 - y/y_c)^a(1 + y/y_1)^{b_1}(y^2/w' + v'y/w' + 1)^{b_2}}, \tag{34}$$

where expressions for the parameters a, b_1, b_2, b_3, c and M are given in the Appendix.

3.2. Model 3—$Y(y)$ represented by a cubic

This model was developed to see to what degree the results were model-sensitive. The cubic representing Y has values $\zeta/\phi^{1/3}$ at $y = 0$, and $\mu y_c/\phi^{1/3}$ at $y = y_c$ and slopes at $y = 0$ and $y = y_c$ of 0 and $\mu/\phi^{1/3}$ respectively. Again, with $\zeta = \mu = 1$ this is a cubic representation of Voorhees' proposal. It is given by

$$Y = \phi^{-1/3}\left[\zeta + y^2\left(\frac{2\mu}{y_c} - \frac{3\zeta}{y_c^2}\right) + y^3\left(\frac{2\zeta}{y_c^3} - \frac{\mu}{y_c^2}\right)\right]. \tag{35}$$

The expression for W is

$$W = \frac{\lambda_0 + \lambda_2 y^2 + \lambda_3 y^3}{\lambda_0 + \lambda_1 y + \lambda_2 y^2 + \lambda_3 y^3}, \tag{36}$$

where

$$\left.\begin{aligned} \lambda_0 &= 1 + \zeta\alpha/\mu \\ \lambda_1 &= -q \\ \lambda_2 &= \alpha\left[2/y_c - 3\zeta/\left(\mu y_c^2\right)\right] \\ \lambda_3 &= \alpha\left[2\zeta/\left(\mu y_c^3\right) - 1/y_c^2\right] \end{aligned}\right\}. \tag{37}$$

The expression for the growth rate now becomes

$$U = \frac{-\lambda_3 y^6 - \lambda_2 y^5 + (\gamma\lambda_3 - \lambda_1)y^4 + [\gamma(\lambda_2 - \lambda_3) - \lambda_0]y^3 - \gamma\lambda_2 y^2 + \gamma\lambda_0 y - \gamma\lambda_0}{y^2(\lambda_0 + \lambda_1 y + \lambda_2 y^2 + \lambda_3 y^3)} \tag{38}$$

The relationships for γ and for y_c given by Equations 28 and 30 depend only on the values at $y = y_c$ of Y and its slope, hence the same expressions are valid for model 3 as for model 2. Deflation of the 6th order polynomial, P_6, in the numerator of Equation 38 by $(y_c - y)^2$ will give a polynomial, P_4, of fourth order which will have four real roots or two real and two complex roots. Only the latter case is of interest for model 3 and the integral in Equation 22 becomes

$$I = \int_0^y \frac{y'^2(\lambda_0 + \lambda_1 y' + \lambda_2 y'^2 + \lambda_3 y'^3)}{-\lambda_3(y_c - y')^2(y' + y'_1)(y' + y'_2)(y'^2 + v'y' + w')}\,dy', \tag{39}$$

where $-y_1$, $-y_2$ are the real roots of P_4 and v' and w' are the coefficients of the quadratic factor.

Using this in Equation 22 gives

$$p' = \frac{3y^2(\lambda_0 + \lambda_1 y + \lambda_2 y^2 + \lambda_3 y^3)\exp\left(\frac{-cy}{y_c - y}\right)\exp\left[M\tan^{-1}\left(\frac{y\sqrt{w' - v'^2/4}}{w' - v'y/2}\right)\right]}{\gamma\lambda_0(1 - y/y_c)^a(1 + y/y_1)^{b_1}(1 + y/y_2)^{b_2}(y^2/w' + v'y/w' + 1)^{b_3}}, \tag{40}$$

where expressions for the parameters a, b_1, b_2, b_3 and M are also give in the Appendix.

3.3. Finding the parameters

We now have expressions for the distribution functions and for the parameters occurring in them for both models. However the expressions are not wholly explicit in terms of ϕ but are given in part implicitly via the sink factor, q (through α and β) which is a function of ϕ. The relationship between q and ϕ is given by Equation 20 but this requires a knowledge of the distribution function, p', in order to calculate the required mean values. A numerical procedure is therefore required to find the parameters for a given ϕ. This is based on Equation 20 regarded as a non-linear equation relating q and ϕ which can be solved iteratively. This involves making estimates of q, and with them calculating y_c and the other roots together with the coefficients of the quadratic factor, then calculating the parameters in the Appendix and using these to calculate a trial distribution function from the appropriate Equation [33, 34 or 40]. The mean values required in Equation 20 can then be found and the values of ϕ corresponding to the values of q can be determined. From these a value of q can be found giving a value of ϕ closer to the target value using the secant method and the process repeated until the calculated ϕ is sufficiently close to the target. The process is efficient and converges rapidly. The input to a program based on this algorithm is the volume fraction, ϕ, and the two parameters, ζ and μ, and the output is the distribution function and all the parameters required for its calculation.

There are three checks available to determine whether the analysis and the numerical results are correct. Firstly Equations 34, 35 and 41 must reduce to the LSW expression in the limit $\phi \to 0$ (for which see below) and the programming should produce the same result numerically. Secondly according to Equation 22, the programming must produce a normalized distribution function without any normalization procedure when C is set to 3. Finally, since we are in the asymptotic condition the distribution function must give $\langle W \rangle = \langle yW \rangle$ according to Equation 6. No distribution which fails any of these three checks can be correct.

3.4. Equations in terms of experimentally observable variables

The variable $y = r/r^*$ is useful for analysis but is of little value for comparison with experiment since r^* is not accessible to measurement. It is important to make the results of theory available to experimenters. The measurable quantity is the mean value, $\langle r \rangle$, and we therefore express the results in terms of the variable $\rho = r/\langle r \rangle$. Using p' we can find $\langle y \rangle = \langle r \rangle / r^*$ and from this find the probability distribution p, where $p\,d\rho$ is the probability of a particle having a relative size in the range ρ to $\rho + d\rho$. The distribution p is given by

$$p = \langle y \rangle p'. \tag{41}$$

We define

$$\left.\begin{aligned} \rho &= y/\langle y \rangle \\ \rho_c &= y_c/\langle y \rangle \\ \rho_1 &= y_1/\langle y \rangle \\ \rho_2 &= y_2/\langle y \rangle \\ \rho_3 &= y_3/\langle y \rangle \\ w &= w'/\langle y \rangle^2 \\ v &= v'/\langle y \rangle \end{aligned}\right\}. \tag{42}$$

It is convenient also to simplify the equations by defining a set of coefficients for the pre-exponential quadratic or cubic in Equations 33, 34 and 40 which incorporate the factors $\langle y \rangle^n$ together with the term λ_0 in the denominator of the equations. These are

$$\left.\begin{aligned} A_0 &= \langle y \rangle^3 \\ A_1 &= \langle y \rangle^4 \lambda_1/\lambda_0 \\ A_2 &= \langle y \rangle^5 \lambda_2/\lambda_0 \\ A_3 &= \langle y \rangle^6 \lambda_3/\lambda_0 \end{aligned}\right\} \tag{43}$$

The parameter M is unchanged in value if ρ, w and v are used in the Equations A5 and A8 in place of y, w' and v'. The parameters a, b_1, b_2, b_3, and c are also unchanged by the transformation of variables. In terms of ρ the equations for the distribution functions become

$$p = \frac{3\rho^2(A_0 + A_1\rho + A_2\rho^2)\exp\left(\frac{-c\rho}{\rho_c - \rho}\right)}{\gamma(1 - \rho/\rho_c)^a(1 + \rho/\rho_1)^{b_1}(1 + \rho/\rho_2)^{b_2}(1 + \rho/\rho_3)^{b_3}}, \tag{44}$$

$$p = \frac{3\rho^2(A_0 + A_1\rho + A_2\rho^2)\exp\left(\dfrac{-c\rho}{\rho_c - \rho}\right)\exp\left[M\tan^{-1}\left(\dfrac{\rho\sqrt{w - v^2/4}}{w - v\rho/2}\right)\right]}{\gamma(1 - \rho/\rho_c)^a(1 + \rho/\rho_1)^{b_1}(\rho^2/w + v\rho/w + 1)^{b_2}} \tag{45}$$

and

$$p = \frac{3\rho^2\left(A_0 + A_1\rho + A_2\rho^2 + A_3\rho^3\right)\exp\left(\dfrac{-c\rho}{\rho_c - \rho}\right)\exp\left[M\tan^{-1}\left(\dfrac{\rho\sqrt{w - v^2/4}}{w - v\rho/2}\right)\right]}{\gamma(1 - \rho/\rho_c)^a(1 + \rho/\rho_1)^{b_1}(1 + \rho/\rho_2)^{b_2}(\rho^2/w + v\rho/w + 1)^{b_3}}. \tag{46}$$

3.5. Limiting cases

There are a number of limiting cases of the Equations 44, 45 and 46 which are of interest. As ϕ approaches zero we find

$$\left.\begin{aligned} &q \to 0, \alpha \to 0, \beta \to 0, \langle y\rangle \to 1, A_0 \to 1, A_1 \to 0, A_2 \to 0, \\ &A_3 \to 0, \rho_1 \to 3, \rho_2 \to \infty, \rho_3 \to \infty, \gamma \to 27/4, \rho_c \to 3/2, \\ &a \to 11/3, b_1 \to 7/3, b_2 \to 1, b_3 \to 1, c \to 1, w \to \infty, \end{aligned}\right\} \tag{47}$$

together with

$$M\tan^{-1}\left(\frac{\rho\sqrt{w - v^2/4}}{w - v\rho/2}\right) \to 0, \tag{48}$$

and, independently of the values of ζ and μ, Equations 44, 45 and 46 all converge to Equation 1 and therefore give, as they must, the LSW result [2, 3].

If we set $\zeta = 0$ and $\mu = 1$ for model 2, Equation 23 then gives $Y = y/\phi^{-1/3}$ and we have Model 1, the self-consistent version proposed by Brailsford and Wynblatt [5]. With ζ close to 0 and μ close to 1, Equation 44 applies and as they approach these values $\rho_3 \to \infty$, $b_3 \to 1$, $A_0 \to \langle y\rangle^3$, $A_1 \to \beta\langle y\rangle^4$, and $A_2 \to 0$. The probability distribution is then

$$p = \frac{3\rho^2(A_0 + A_1\rho)\exp\left(\dfrac{-c\rho}{\rho_c - \rho}\right)}{\gamma(1 - \rho/\rho_c)^a(1 + \rho/\rho_1)^{b_1}(1 + \rho/\rho_2)^{b_2}}, \tag{49}$$

where the expressions for the parameters required are also given in the Appendix.

If we set $\zeta = 0$ and $\mu = \phi^{1/3}$ in model 2 then $Y = y$ and we have the original version of Brailsford and Wynblatt [5]. With ζ and μ near these values Equation 45 applies and $\rho_2 \to \infty$, $b_2 \to 1$, $A_0 \to \langle y\rangle^3$, $A_1 \to 0$, $A_2 \to 0$, and the second exponential approaches 1. The probability distribution then becomes

$$p = \frac{3\rho^2\langle y\rangle^3\exp\left(\dfrac{-c\rho}{\rho_c - \rho}\right)}{\gamma(1 - \rho/\rho_c)^a(1 + \rho/\rho_1)^{b_1}}. \tag{50}$$

Expressions for the parameters are given by Brailsford and Wyblatt [5].

In addition to the original Brailsford and Wynblatt model we have now produced three new models of the coarsening process, only one of which is self-consistent. The next task is to produced self-consistent versions of models 2 and 3.

4. Self-consistent versions of models 2 and 3

The generalised definition of self-consistency has already been given as equality of the volume fraction, ϕ, with the mean value, ϕ_a, of the ratio of particle volume to averaging sphere volume, and once a solution has been obtained for particular values of ϕ, ζ and μ, the distribution function is available to calculate ϕ_a. One way in which self-consistency can be achieved is to set $\zeta = 1$ and find the value of μ (between $\phi^{1/3}$ and 1) which makes $\phi_a = \phi$. This is shown schematically in Fig. 3. As discussed in Section 3 in connection with the Voorhees' suggestion, when $\mu < 1$, part of the Y curve at large y lies below the line $Y = y/\phi^{1/3}$ and particles

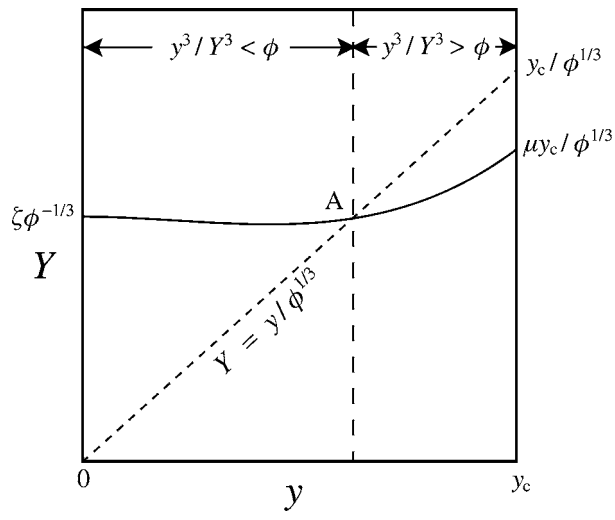

Figure 3 Illustrating how the value of μ is changed to make the average ratio of particle volume to averaging sphere volume equal to the volume fraction, ϕ. For particles to the left of A this ratio is less than ϕ, for particles to the right of A it is greater than ϕ and a correct choice of μ will make the average equal to ϕ.

in this region make a contribution to ϕ_a which is greater than ϕ while particles in the region where the curve lies above the line, make a contribution less than ϕ.

The value of μ required to make $\phi_a = \phi$ is found by putting an outer iterative loop around the one which finds the distribution function for given ϕ, ζ, and μ as described in Section 5. After setting $\zeta = 1$, trial values of μ are used to determine the probability distribution and the corresponding values of ϕ_a, the secant method again being used to choose a value for μ making the difference $\phi - \phi_a$ closer to zero. Rapid convergence is achieved. The input to such a procedure is ϕ only, since ζ is pre-set and μ is determined by the procedure itself.

There is an upper limit, ϕ_m, to the volume fraction to which this method may be applied since μ cannot be less than $\phi^{1/3}$ or the averaging sphere radius would be less than the particle radius for large particles. For Model 2 this upper limit is $\phi_m \approx 0.4454$ and for Model 3, $\phi_m \approx 0.3638$.

We now have three self-consistent versions of the theory; version 1, the Brailsford and Wynblatt proposal, and versions 2 and 3, being models 2 and 3 treated by the method described above. In order to make the results available for comparison with experiment, Tables I, II and III are provided. These list the parameters required for use in Equations 49, 45, and 46 to evaluate the distribution functions for a range of volume fractions for each of these versions. Table IV also lists the parameters required for the evaluation of the original Brailsford and Wynblatt [5] version (Equation 50). Linear interpolation to find parameters for volume fractions not in the tables is reasonably accurate for volume fractions not too close to zero. This makes it possible to compare theoretical distribution functions with experimental results. The authors will supply computer programs to evaluate the parameters as a function of volume fraction on request.

Finally we are now in a position to provide the parameters in the equivalent of Equation 2 for a finite volume fraction. Integrating Equation 18 using $\langle r \rangle$ in place of r^* gives

$$\langle r \rangle^3 - \langle r_0 \rangle^3 = \frac{3K \langle y \rangle^3}{\gamma} t = k(\phi)t, \qquad (51)$$

where $\langle r_0 \rangle$ is the mean particle radius at $t = 0$ and $k(\phi)$ is the rate constant at volume fraction, ϕ. The values of γ and $\langle y \rangle$ required for use in this equation can be found from Tables I to IV.

5. Results

Before looking at the distribution functions for the self-consistent versions, it is worth while gaining an impression of the effects of ζ and μ separately. Fig. 4 shows the distribution functions for a volume fraction of 0.3 using model 3. The upper set of curves show the effect of μ when the parameter ζ is held constant at 1. (For convenience in this figure, μ' is μ scaled so that it runs from 0 to 1 instead of from $\phi^{1/3}$ to 1, hence $\mu' = 0$ is equivalent to $\mu = \phi^{1/3}$, the smallest possible value of μ.) The lower set of curves show the effect of the other parameter, ζ, with μ held at 1. It can be verified from Fig. 4 that, roughly speaking, lowering μ makes the averaging sphere smaller for the larger particles while reducing ζ does the same for the smaller particles.

It is clear that μ has a more significant effect on the distribution functions than ζ. When μ is reduced the distributions become broader, less peaked and more symmetrical. The opposite effect is found with ζ, a reduction of which makes the distributions narrower, more strongly peaked and somewhat more skewed. However, as noted, the effect of ζ is less pronounced. The effect of both together is found in the original model

TABLE I Parameters for the calculation of the particle size probability distribution for the first self-consistent version as a function of volume fraction for use in Equation 49. This version represents the relative averaging sphere radius as a linear function of relative particle radius

ϕ	q	A_0	A_1	a	b_1	b_2	c	ρ_c	ρ_1	ρ_2	γ	$\langle y \rangle$
0	0	1	0	11/3	7/3	1	1	3/2	3	∞	27/4	1
10^{-6}	0.00163	0.99983	0.16242	3.6684	2.3220	1.0096	1.0015	1.5005	2.9850	6.2100	6.7367	0.99942
10^{-4}	0.01640	0.99866	0.33632	3.6761	1.5685	1.7554	1.0095	1.5034	2.5510	3.4251	6.6414	0.99951
10^{-3}	0.05247	0.99643	0.47001	3.6869	1.1802	2.1328	1.0225	1.5083	1.8185	3.3181	6.4523	0.99881
0.005	0.11964	0.99300	0.57461	3.7003	1.1185	2.1812	1.0404	1.5155	1.3812	3.3780	6.1578	0.99766
0.01	0.17159	0.99061	0.61703	3.7085	1.1040	2.1874	1.0621	1.5204	1.2183	3.4279	5.9565	0.99686
0.02	0.24745	0.98735	0.65298	3.7190	1.0929	2.1882	1.0675	1.5269	1.0685	3.4974	5.6887	0.99576
0.04	0.35976	0.98278	0.67334	3.7326	1.0838	2.1836	1.0886	1.5359	0.92964	3.5952	5.3322	0.99423
0.06	0.45020	0.97923	0.68047	3.7429	1.0790	2.1781	1.1048	1.5428	0.85255	3.6721	5.0708	0.99303
0.08	0.52957	0.97615	0.67730	3.7515	1.0759	2.1726	1.1188	1.5488	0.79931	3.7396	4.8566	0.99199
0.10	0.60203	0.97336	0.67043	3.7593	1.0735	2.1672	1.1315	1.5543	0.75866	3.8018	4.6715	0.99104
0.12	0.66974	0.97076	0.66140	3.7665	1.0716	2.1619	1.1434	1.5594	0.72577	3.8608	4.5066	0.99016
0.14	0.73397	0.96829	0.65097	3.7734	1.0700	2.1566	1.1547	1.5643	0.69812	3.9179	4.3567	0.98931
0.16	0.79555	0.96590	0.63959	3.7800	1.0687	2.1513	1.1656	1.5690	0.67424	3.9739	4.2186	0.98850
0.18	0.85509	0.96359	0.62754	3.7864	1.0675	2.1461	1.1764	1.5736	0.65319	4.0294	4.0898	0.98771
0.20	0.91299	0.96133	0.61500	3.7928	1.0664	2.1408	1.1869	1.5781	0.63435	4.0850	3.9687	0.98694
0.22	0.96960	0.95910	0.60207	3.7991	1.0654	2.1355	1.1975	1.5826	0.61727	4.1409	3.8542	0.98618
0.24	1.0252	0.95689	0.58885	3.8054	1.0651	2.1301	1.2079	1.5870	0.60162	4.1974	3.7452	0.98452
0.26	1.0799	0.95470	0.57539	3.8117	1.0637	2.1246	1.2185	1.5915	0.58717	4.2550	3.6410	0.98466
0.28	1.1340	0.95251	0.56174	3.8181	1.0629	2.1190	1.2291	1.5960	0.57373	4.3138	3.5412	0.98391
0.30	1.1876	0.95318	0.54793	3.8246	1.0622	2.1132	1.2398	1.6005	0.56114	4.3741	3.4450	0.98316
0.32	1.2409	0.94812	0.53399	3.8311	1.0615	2.1074	1.2507	1.6050	0.54929	4.4363	3.3521	0.98240
0.34	1.2939	0.94591	0.51992	3.8378	1.0609	2.1013	1.2618	1.6096	0.53809	4.5005	3.2621	0.91164

TABLE II Parameters for the calculation of the particle size probability distribution for the second self-consistent version as a function of volume fraction for use in Equation 45. This version represents the relative averaging sphere radius as a quadratic function of relative particle radius

ϕ	q	A_0	$-A_1$	A_2	a	b_1	b_2	c
0	0	1	0	0	11/3	7/3	1	1
10^{-6}	0.0016309	0.99981	0.065000	0.062265	3.6680	2.3328	0.99961	1.0015
10^{-4}	0.016401	0.99843	0.12995	0.11529	3.6708	2.3318	0.99868	1.0091
10^{-3}	0.052487	0.99555	0.18823	0.15037	3.6668	2.3312	1.0010	1.0203
0.005	0.11972	0.99067	0.25134	0.17691	3.6491	2.3303	1.0103	1.0338
0.01	0.17177	0.98704	0.28789	0.18829	3.6312	2.3292	1.0198	1.0414
0.02	0.24787	0.98177	0.33236	0.19918	3.6008	2.3271	1.0361	1.0502
0.04	0.36075	0.97385	0.38671	0.20893	3.5480	2.3229	1.0646	1.0600
0.06	0.45190	0.96723	0.42385	0.21363	3.4993	2.3188	1.0909	1.0658
0.08	0.53210	0.96119	0.45275	0.21620	3.4521	2.3148	1.1166	1.0698
0.10	0.60553	0.95544	0.47659	0.21658	3.4052	2.3106	1.1421	1.0725
0.12	0.67435	0.94983	0.49690	0.21816	3.3580	2.3065	1.1678	1.0744
0.14	0.73985	0.94427	0.51453	0.21813	3.3098	2.3023	1.1939	1.0756
0.16	0.80288	0.93869	0.53003	0.21763	3.2605	2.2980	1.2208	1.0762
0.18	0.86404	0.93303	0.54374	0.21761	3.2095	2.2937	1.2484	1.0763
0.20	0.92380	0.92725	0.55590	0.21542	3.1565	2.2892	1.2771	1.0759
0.22	0.98250	0.92130	0.56665	0.21377	3.1012	2.2846	1.3071	1.0750
0.24	1.0404	0.91513	0.57612	0.21178	3.0432	2.2800	1.3385	1.0737
0.26	1.0979	0.90870	0.58435	0.20943	2.9819	2.2751	1.3715	1.0719
0.28	1.1550	0.90193	0.59138	0.20669	2.9167	2.2700	1.4066	1.0697
0.30	1.2121	0.89477	0.59717	0.20354	2.8470	2.2467	1.4442	1.0669
0.32	1.2693	0.88710	0.60168	0.19991	2.7716	2.2591	1.4846	1.0636
0.34	1.3269	0.87881	0.60477	0.19573	2.6892	2.2532	1.5288	1.0597

ϕ	ρ_c	ρ_1	$-v$	w	M	γ	$\langle y \rangle$
0	3/2	3		∞	0	27/4	1
10^{-6}	1.5005	2.9943	1.0372	16.048	0.0036548	6.7364	0.99994
10^{-4}	1.5037	2.9592	1.0790	8.6033	0.030341	6.6366	0.99948
10^{-3}	1.5096	2.8948	1.1274	6.4871	0.082103	6.4351	0.99852
0.005	1.5186	2.7987	1.1822	5.3570	0.16242	6.1165	0.99688
0.01	1.5249	2.7343	1.2134	4.9250	0.21797	5.8963	0.99566
0.02	1.5338	2.6494	1.2504	4.5111	0.29332	5.6006	0.99389
0.04	1.5469	2.5369	1.2941	4.1016	0.39679	5.2020	0.99121
0.06	1.5576	2.4544	1.3233	3.8569	0.47526	4.9059	0.98896
0.08	1.5673	2.3863	1.3457	3.6773	0.54135	4.6605	0.98689
0.10	1.5766	2.3270	1.3641	3.5327	0.59974	4.4461	0.98492
0.12	1.5858	2.2737	1.3799	3.4099	0.65274	4.2532	0.98299
0.14	1.5949	2.2247	1.3938	3.3019	0.70166	4.0758	0.98107
0.16	1.6041	2.1790	1.4062	3.2045	0.74736	3.9104	0.97913
0.18	1.6137	2.1358	1.4175	3.1151	0.79037	3.7543	0.97716
0.20	1.6235	2.0945	1.4280	3.0318	0.83107	3.6056	0.97514
0.22	1.6338	2.0547	1.4377	2.9532	0.86970	3.4628	0.97305
0.24	1.6448	2.0162	1.4470	2.8783	0.90642	3.3248	0.97087
0.26	1.6565	1.9785	1.4558	2.8062	0.94131	3.1904	0.86859
0.28	1.6691	1.9414	1.4644	2.7363	0.97440	3.0588	0.96618
0.30	1.6828	1.9046	1.4728	2.6680	1.0056	2.9290	0.96361
0.32	1.6981	1.8678	1.4813	2.6005	1.0348	2.8001	0.96085
0.34	1.7153	1.8308	1.4901	2.5334	1.0618	2.6710	0.95785

of Brailsford and Wynblatt [5] which sets $Y = y$, the equivalent of setting $\mu = \phi^{1/3}$ and $\zeta = 0$ in model 2. This produces distributions which are broadened but also more strongly skewed than the curve in Fig. 4 with $\mu = \phi^{1/3}$ ($\mu' = 0$) might suggest.

Distribution functions for the three self-consistent versions over similar ranges of volume fraction are shown in Figs. 5 to 7. Those of versions 2 and 3 are superficially very similar while those of version 1, the self-consistent Brailsford and Wynblatt proposal, are markedly different in a way which could be anticipated from the effects of ζ and μ on the distributions as seen in Figs 4a and b. They change much less rapidly with volume fraction and are more highly peaked, narrower and more skewed than the distributions of versions 2 and 3. A closer comparison is provided in Fig. 8 which shows the distributions for volume fractions of 0.1 and 0.2 on the same plots, including also the distributions for the original Brailsford and Wynblatt model which is not self-consistent, having $Y = y$ and identified by BW in this and subsequent figures. Versions 2 and 3 are, as expected, very similar. Their peak heights lie below that of version 1 but above that of BW. All the curves would be identical at $\phi = 0$ and the difference between versions 1, 2 and 3 do appear to be less at the smaller volume fraction. The distribution curves for the BW version, however, appear to vary more rapidly at small volume fractions. Although the difference between the curves for versions 2 and 3 are small, those for version 3 are a little broader and somewhat less sharply peaked than those of version 2. This is the case over the whole applicable volume fraction range for the two versions.

TABLE III Parameters for the calculation of the particle size probability distribution for the third self-consistent version as a function of volume fraction for use in Equation 46. This version represents the relative averaging sphere radius as a cubic function of relative particle radius

ϕ	q	A_0	$-A_1$	$-A_2$	A_3	a	b_1	b_2	b_3
0	0	1	0	0	0	11/3	7/3	1	1
10^{-6}	0.001631	0.99981	0.0014183	0.029656	0.030630	3.6677	1.2989	2.0337	0.9999
10^{-4}	0.016401	0.99838	0.012093	0.055676	0.056834	3.6650	1.0777	2.2507	1.0033
10^{-3}	0.052487	0.99532	0.034206	0.072379	0.073720	3.6449	1.1045	2.2169	1.0171
0.005	0.11973	0.99008	0.069490	0.084790	0.085994	3.5939	1.1467	2.1628	1.0483
0.01	0.17177	0.98163	0.093809	0.090010	0.090977	3.5486	1.1749	2.1268	1.0749
0.02	0.24788	0.98034	1.26178	0.094904	0.095423	3.4761	1.2128	2.0784	1.1635
0.04	0.36079	0.97153	1.68937	0.099120	0.098832	3.3576	1.2651	2.0117	1.1828
0.06	0.45198	0.96408	1.99800	1.01010	0.099978	3.2334	1.3056	1.9602	1.2404
0.08	0.53223	0.95721	2.24626	1.01921	0.10018	3.1557	1.3407	1.9158	1.2939
0.10	0.60574	0.94733	2.45624	1.02266	0.099828	3.0614	1.3727	1.8755	1.3452
0.12	0.67465	0.94408	2.63884	1.02223	0.099096	2.9689	1.4027	1.8378	1.3953
0.14	0.74028	0.93754	2.80037	1.01876	0.098063	2.8770	1.4314	1.8018	1.4449
0.16	0.80347	0.93090	2.94477	1.01127	0.096769	2.7848	1.4594	1.7670	1.4944
0.18	0.86484	0.92407	3.07463	1.00427	0.095231	2.6917	1.4868	1.7328	1.5444
0.20	0.92485	0.91700	3.19169	0.99348	0.093449	2.5969	1.5141	1.7000	1.5950
0.22	0.98388	0.90956	3.29706	0.98022	0.091401	2.4998	1.5415	1.6650	1.6468
0.24	1.04223	0.90169	3.39138	0.97259	0.089087	2.4000	1.5693	1.6307	1.7002
0.26	1.10019	0.89325	3.47482	0.94506	0.086435	2.2950	1.5978	1.5956	1.7558
0.28	1.15802	0.88407	3.54706	0.92196	0.083379	2.1845	1.6276	1.5590	1.8144
0.30	1.21600	0.87387	3.60706	0.89366	0.079795	2.0657	1.6593	1.5203	1.8774
0.32	1.27440	0.86218	3.65247	0.85777	0.075457	1.9340	1.6940	1.4778	1.9471
0.34	1.22271	0.84802	3.67773	0.80900	0.066976	1.7791	1.7346	1.4286	2.0289

ϕ	c	ρ_c	ρ_1	ρ_2	$-v$	w	M	γ	$\langle y \rangle$
0	1	3/2	3	∞		∞	0	27/4	1
10^{-6}	1.0014	1.5005	2.8639	3.0405	3.8716	11.218	0.003513	6.7363	0.99994
10^{-4}	1.0084	1.5038	2.2800	3.0246	3.2785	7.4790	0.032413	6.6349	0.99946
10^{-3}	1.0172	1.5100	2.0511	3.0233	3.0362	6.1679	0.091598	6.4289	0.99844
0.005	1.0254	1.5196	1.9079	3.0131	2.8678	5.3446	0.18499	6.1014	0.99668
0.01	1.0285	1.5265	1.8489	3.0036	2.7889	4.9897	0.04917	5.8741	0.99535
0.02	1.0298	1.5362	1.7900	2.9894	2.7015	4.6205	0.33455	5.5679	0.99341
0.04	1.0273	1.5507	1.7294	2.9692	2.6000	4.2226	0.44689	5.1532	0.99042
0.06	1.0220	1.5629	1.6184	2.9544	2.5307	3.9682	0.52695	4.8437	0.98788
0.08	1.0153	1.5742	1.6636	2.9427	2.4754	3.7737	0.58999	4.5859	0.98553
0.10	1.0077	1.5851	1.6403	2.9333	2.4279	3.6126	0.64166	4.3597	0.98325
0.12	0.99913	1.5960	1.6299	2.9259	2.3854	3.4726	0.68470	4.1550	0.98100
0.14	0.98979	1.6072	1.6018	2.9201	2.3465	3.3472	0.72064	3.9658	0.97873
0.16	0.97965	1.6187	1.5851	2.9160	2.3101	3.2323	0.75034	3.7881	0.97641
0.18	0.96869	1.6309	1.5693	2.9136	2.2756	3.1252	0.74278	3.6193	0.97402
0.20	0.95685	1.6439	1.5542	2.9130	2.2425	3.0239	0.79264	3.4571	0.97153
0.22	0.94405	1.6579	1.5396	2.9144	2.2105	2.9269	0.85401	3.2997	0.96890
0.24	0.93016	1.6734	1.5252	2.9182	2.1791	2.8329	0.81228	3.1455	0.96609
0.26	0.91501	1.6907	1.5110	2.9251	2.1481	2.7406	0.81273	2.9928	0.96307
0.28	0.89834	1.7106	1.4968	2.9359	2.1172	2.6488	0.80575	2.8398	0.95976
0.30	0.87974	1.7342	1.4822	2.9523	2.0861	2.5559	0.78963	2.6841	0.95602
0.32	0.85850	1.7636	1.4670	2.9777	2.0542	2.4594	0.76114	2.5215	0.95177
0.34	0.83312	1.8038	1.4507	3.0195	2.0207	2.3545	0.71293	2.3440	0.9465

An alternative way of investigating the shape of the size distributions is to look at statistical parameters such as standard deviations and coefficients of skewness as well as the upper cut-off size, ρ_c. Plots of standard deviation, s, are shown in Fig. 9 and skewness, k_s, in Fig. 10. The point made previously that the distributions of the BW version vary more rapidly at small ϕ than any of the self-consistent versions is clear from these two figures. For the self-consistent versions, 2 and 3 are very similar as expected and, at low ϕ, have values of s and k_s varying more rapidly than those of version 1. In all versions the absolute value of skewness decreases with increasing ϕ (note that $-k_s$ is plotted in Fig. 10). This observation reinforces the point already made in connection with the distribution functions shown in Figs 5 to 8. The changes in width of the distributions, also evident in the same figures, is shown in the plots of the relative particle cut-off size, ρ_c versus ϕ in Fig. 11 although in some cases the ρ axis in Figs 5 to 8 does not extend to ρ_c since there may be a long tail in which p is indistinguishable from zero at the chosen scale.

In Figs 9 and 10 are plotted values of standard deviation and skewness for a value of $\phi = 0.1$ taken from the numerical simulations of Akaiwa and Voorhees [22], which is probably the most complete work of this kind in the sense of dealing with most of the factors affecting the coarsening process. It can be seen that these are very close to the values from the simple Brailsford and Wynblatt model. This is surprising, but without more complete data it would be premature to draw any conclusions.

The effect of volume fraction on the kinetics of growth given by the ratio of the rate constant in Equation 51 (the factor multiplying t) at a particular volume

TABLE IV Parameters for the calculation of the particle size probability distribution for the original Brailsford and Wynblatt (non-self-consistent) version as a function of volume fraction for use in Equation 50. This version sets the relative averaging sphere radius equal to the relative particle radius

ϕ	q	a	b_1	c	ρ_c	ρ_1	γ	$\langle y \rangle$
0	1	11/3	7/3	1	3/2	3	27/4	1
10^{-6}	0.0016311	3.6699	2.3301	1.0024	1.5007	2.9905	6.7335	0.99992
10^{-4}	0.016436	3.6992	2.3008	1.0246	1.5073	2.9062	6.5873	0.99924
10^{-3}	0.052944	3.7690	2.2310	1.0783	1.5230	2.7143	6.2505	0.99759
0.005	0.12240	3.8924	2.1706	1.1771	1.5516	2.4028	5.6907	0.99456
0.01	0.17748	3.9814	2.0186	1.2519	1.5730	2.1964	5.3093	0.99226
0.02	0.25999	4.1010	1.8990	1.3577	1.6031	1.9390	4.8203	0.98898
0.04	0.38637	4.2548	1.7452	1.5048	1.6449	1.6344	4.2175	0.98431
0.06	0.94143	4.3594	1.6406	1.6137	1.6761	1.4400	3.8163	0.98074
0.08	0.58570	4.4012	1.5629	1.7017	1.7017	1.2983	3.5141	0.97776
0.10	0.67323	4.5005	1.4995	1.7759	1.7235	1.1879	3.2721	0.97516
0.12	0.75606	4.5515	1.4485	1.8401	1.7426	1.0984	3.0712	0.97284
0.14	0.83540	4.5942	1.4058	1.8966	1.7597	1.0238	2.8999	0.97073
0.16	0.91205	4.6303	1.3697	1.9469	1.7752	0.96020	2.7513	0.96880
0.18	0.98652	4.6614	1.3386	1.9922	1.7893	0.90518	2.6205	0.96702
0.20	1.0592	4.6884	1.3116	2.0332	1.8022	0.85696	2.5040	0.96535
0.22	1.1304	4.7121	1.2879	2.0706	1.8142	0.81426	2.3993	0.96379
0.24	1.2004	4.7330	1.2670	2.1050	1.8254	0.77610	2.3046	0.96232
0.26	1.2692	4.7516	1.2484	2.1367	1.8358	0.74175	2.2182	0.96094
0.28	1.3372	4.7682	1.2319	2.1660	1.8456	0.71063	2.1390	0.95962
0.30	1.4042	4.7830	1.2170	2.1932	1.8548	0.68227	2.0661	0.96837
0.32	1.4706	4.7965	1.2035	2.2186	1.8635	0.65630	1.9987	0.95718
0.34	1.5363	4.8087	1.1913	2.2424	1.8717	0.63241	1.9360	0.95605

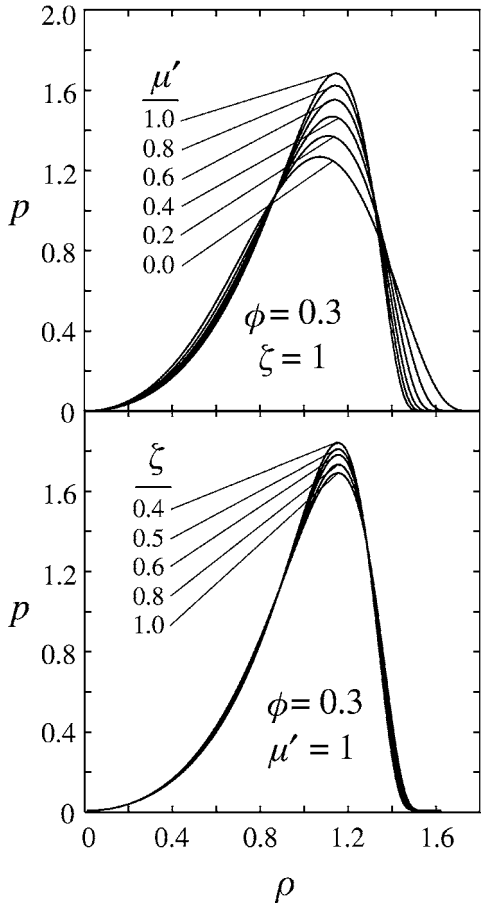

Figure 4 Illustrating the effects of ζ and μ on the particle size probability distributions at a volume fraction of 0.3.

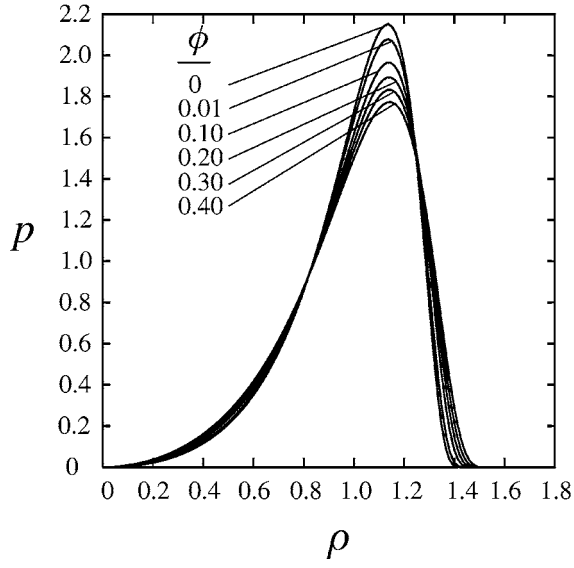

Figure 5 Particle size probability distributions at various volume fractions for the first self-consistent version in which the averaging sphere is a linear function of the particle radius.

fraction to the rate constant at zero volume fraction. This is usually called the k-ratio, $k(\phi)/k(0)$ and is given by

$$\frac{k(\phi)}{k(0)} = \frac{27\langle y \rangle_\phi^3}{4\gamma_\phi}, \qquad (52)$$

where the subscript ϕ indicates values at the appropriate volume fraction ($\gamma_0 = 27/4$, $\langle y \rangle_0 = 1$). This is plotted in Fig. 12. The ratios for versions 2 and 3 are very similar up to $\phi \approx 0.2$ and and only slightly greater than that for version 1. The BW versions gives a greater k-ratio and thus predicts faster average growth rates than any of the self-consistent versions.

The results of theories which do not take spatial correlations into account are not expected to be accurate beyond volume fractions of 0.15 to 0.2. A noticeable feature of Figs 9 to 12 is that the rate of change with volume fraction of the property concerned, (s, k_s ρ_c and k-ratio) for versions 2 and 3 increases markedly in absolute value as the upper volume fraction limit, ϕ_m, is approached, often causing an intersection with the

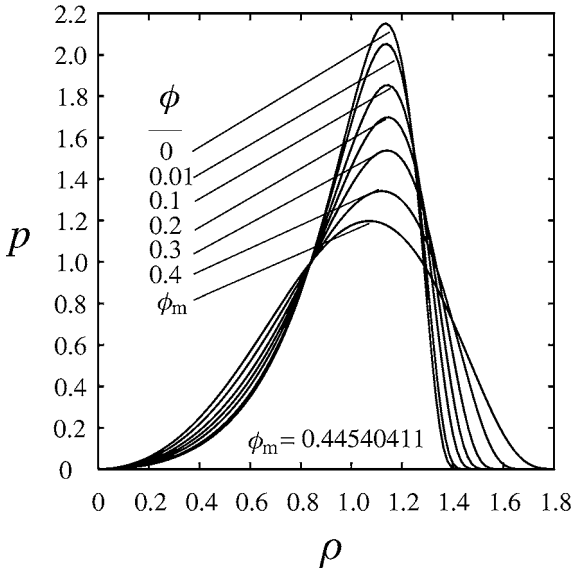

Figure 6 Particle size probability distributions at various volume fractions for the second self-consistent version in which the averaging sphere is a quadratic function of particle size. ϕ_m is the upper limiting volume fraction for this model.

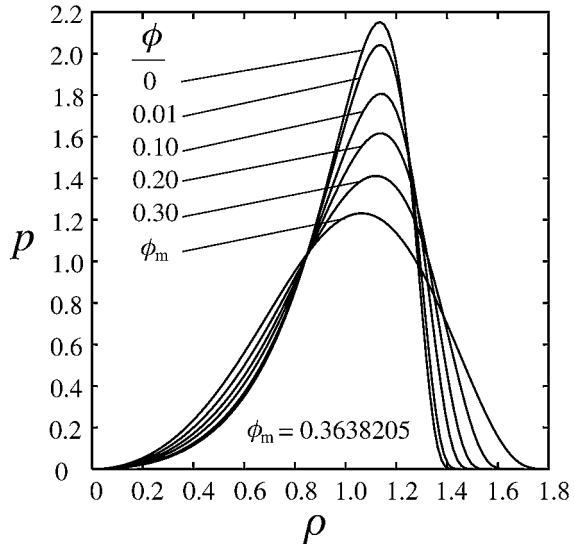

Figure 7 Particle size probability distributions at various volume fractions for the third self-consistent version in which the averaging sphere radius is a cubic function of particle size. ϕ_m is the upper limiting volume fraction for this model.

BW curve. This occurs at a volume fraction of about 0.25 for version 2 and about 0.2 for version 3 and corresponds with an effect which can be seen in the distribution functions (Figs 6 and 7) the peak positions of which move to the left as the volume fraction approaches ϕ_m for both versions. However, this behaviour is outside the range where the results can be expected to apply.

6. Discussion

The different mean growth rate or mean field theories all use different techniques for finding the mean value. They can be very conveniently compared using the $W(y, \phi)$ function, which, as has been noted, is the factor converting the zero volume fraction growth rate to that for a finite volume fraction. The treatment of Marqusee

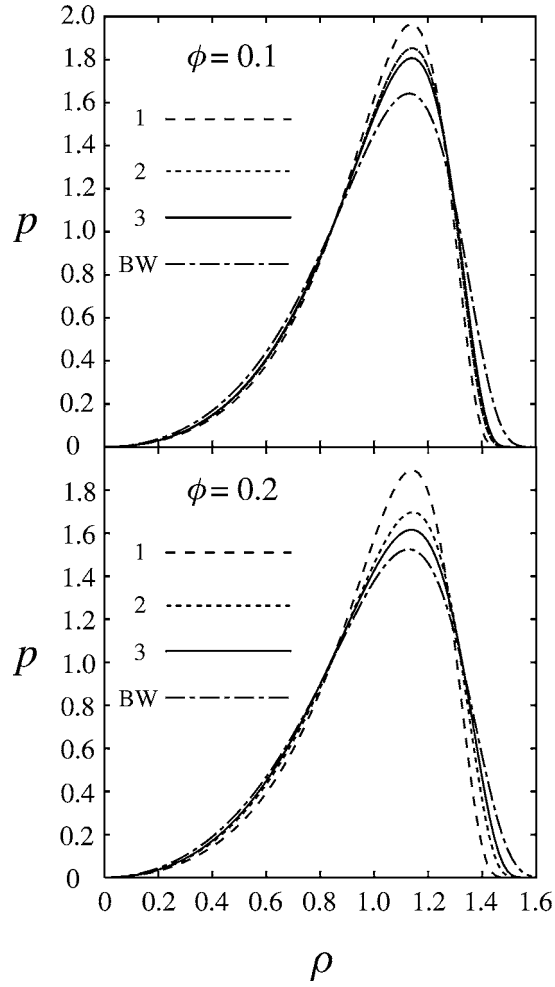

Figure 8 Comparison of the particle size probability distribution functions for three self-consistent versions (labelled 1, 2 and 3) at volume fractions of 0.1 and 0.2 together with the distributions of the original Brailsford and Wynblatt version (labelled BW) which is not self-consistent.

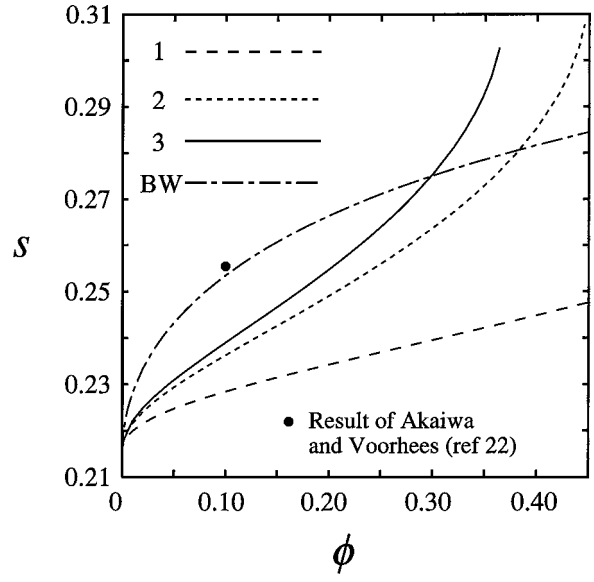

Figure 9 Standard deviation, s, as a function of volume fraction for the three self-consistent versions and the original Brailsford and Wynblatt version (labelling as for Fig. 8).

and Ross [12] involved finding an average growth rate from the formal solution of the multi-particle diffusion problem. They find, with the symbols translated into those of the present paper,

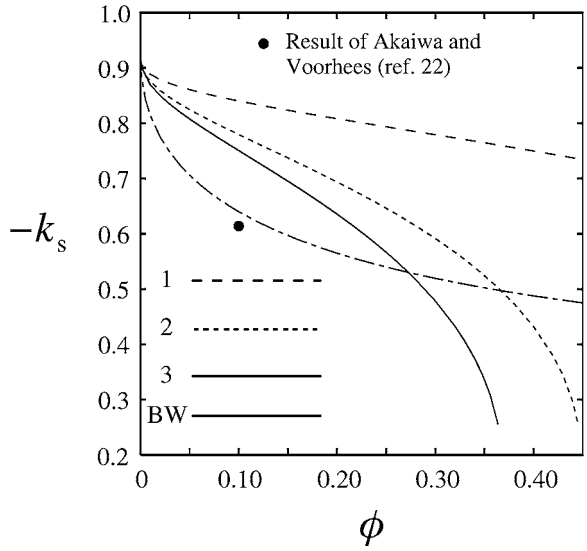

Figure 10 Skewness, k_s, as a function of volume fraction for the three self-consistent versions and the original Brailsford and Wynblatt version (labelling as for Fig. 8).

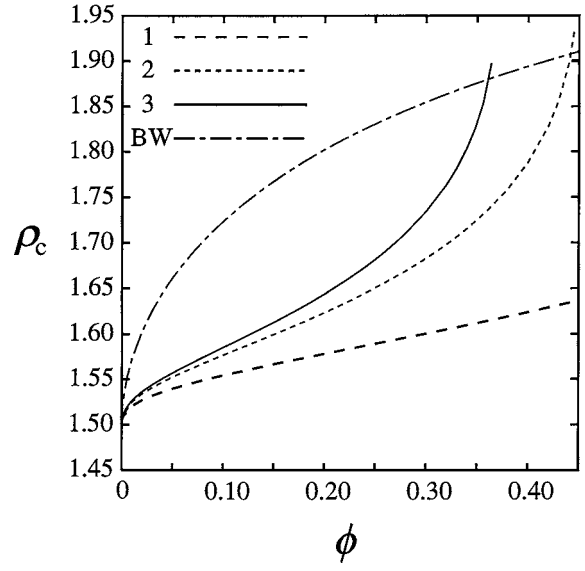

Figure 11 The cut-off value of the relative particle size, ρ_c, as a function of volume fraction for all three self-consistent versions and the original Brailsford and Wynblatt version (labelling as for Fig. 8).

$$W = 1 + r\sqrt{4\pi n\langle r\rangle}$$
$$= 1 + q'y = 1 + [q\sqrt{\langle y\rangle/\langle yW\rangle}]y, \quad (53)$$

where the first expression is that given by the authors quoted and the second and third have been found from it using $n = 3\phi/(4\pi r^{*3}\langle y^3\rangle)$ together with Equation 20. This form for W is very close to that of the original Brailsford and Wynblatt model [5] in which $W = 1 + qy$ and for which the distribution function is given by Equation 50. Since both $\langle y\rangle$ and $\langle W\rangle$ approach 1 as ϕ becomes small, the results of Marqusee and Ross and of Brailsford and Wynblatt [5] are very close in the volume fraction range in which they are expected to have the greatest validity.

The theory of Tokuyama *et al.* [13–16] can be similarly compared. From the expression for B given by Enomoto *et al.* [15] their expression for W (ignoring

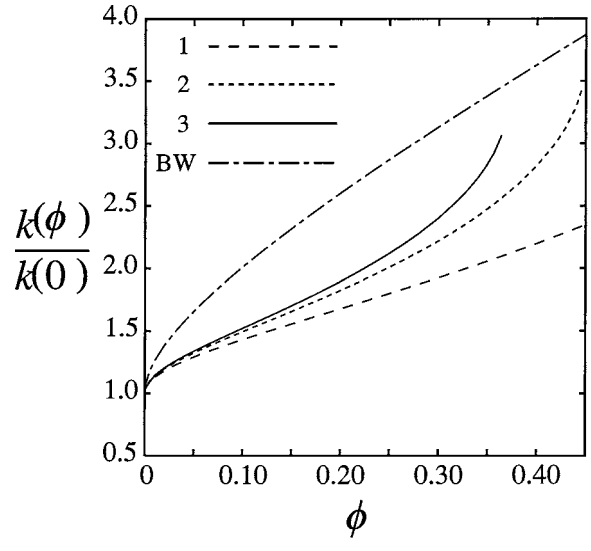

Figure 12 The ratio of the rate constant at a volume fraction, ϕ to the value for zero volume fraction (the k-ratio) as a function of volume fraction for the three self-consistent versions and for the original Brailsford and Wynblatt version (labelling as for Fig. 8).

the so-called soft collision terms) is

$$W = \frac{A_2y^2 + A_1y - 1}{y - 1}, \quad (54)$$

where $A_2 = q'/\langle y\rangle$ and $A_1 = 1/\langle y\rangle - q'\langle y^2\rangle/\langle y\rangle^2$ with q' defined by Equation 53. This would be identical to the Brailsford and Wynblatt result if $A_2 = q$ and $A_1 = 1 - q$ and it can be seen that the results are again closely similar, particularly at low volume fractions.

The results of Yao *et al.* [8] can be treated in a similar manner. Their W function is based on a screening length, ξ', and is

$$W = \exp(r/\xi'), \quad (55)$$

where

$$(\xi')^{-2} = 4\pi n\langle rW\rangle = \frac{3\phi\langle yW\rangle}{r^{*2}\langle y^3\rangle} \quad (56)$$

and comparison with Equation 20 shows that $r^{*2}/\xi'^2 = q^2$ giving $W = e^{qy}$. At small values of q and therefore of ϕ, this also reduces to $W = 1 + qy$, the expression of Brailsford and Wynblatt [5]. Table IV shows, however, that the Brailsford and Wynblatt q is only small enough to justify linearising the exponential for volume fractions less than around 0.001 so the range of ϕ for which there is close coincidence with the original Brailsford and Wynblatt theory will be rather smaller than for the theories of Marqusee and Ross [12] and Enomoto *et al.* [15].

The fact that three theories [5, 12, 15] which use very different methods for averaging the effect of the environment produce very similar results is striking as has been noted by Voorhees [25]. A fourth theory [8] also produces similar results but in a more restricted volume fraction range. This can regarded as confirmation of one aspect of the chemical rate theory model, namely the properties of the effective medium. The value of q and its relation to volume fraction and to the particle size

distribution correspond well with the results obtained by entirely different methods. However, nothing in the three alternatives [5, 12, 15] to the general Brailsford and Wynblatt theory corresponds to the matrix shell around the representative particle giving rise to a W function of the form given by Equation 21. Notwithstanding this, it it has already been noted that the one region in the system where smearing the particles out into a continuum is least appropriate is the immediate vicinity of the representative particle. It is here that the heterogeneous nature of the microstructure is most important. In this region there are no sources or sinks other than the particle itself, and the concentration gradient here determines the particle growth rate. Marqusee's and Ross's procedure [12] to find the mean growth rate assumed amongst other things that particle positions are independent. This probably produces little error in the properties of the effective medium remote from the particle of interest, but the particle overlap which it implies will almost certainly have a very significant effect close to the representative particle. The idea of a matrix shell around the particle separating its surface from the effective medium is a very plausible element in the model for the determination of the mean growth rate for particles in a particular size class.

The chemical rate theory, however, provides little or no basis for a choice of the radius of the matrix shell. Making the model self-consistent, as this has been defined, sets some constraints on the choice, but clearly self-consistency is not enough in itself. This apparent disadvantage may actually be turned into an advantage. Numerical simulation can take into account many more of the features of the complex problem of Ostwald ripening than can be dealt with by an analytical theory of the kind described herein. Numerical simulation is, however, computationally expensive and its results are relatively inaccessible to anyone wishing to compare them with experiment. An analytical theory with sufficient flexibility to allow it to be tuned to produce the same results as numerical simulation over a reasonable range of parameters will make those results more readily available and much more efficient to incorporate in wider theories of, say, the effect of microstructural instability on high temperature mechanical properties. The developmental path which the work reported here points to for the chemical rate theory could well be very useful indeed.

Almost all of the experimental results available currently are for solid/solid systems in which the results may be significantly affected by anisotropy of the surface energy and the generation of internal stresses due to volume changes on transformation. However, experiments on systems with solid particles in a liquid matrix under micro-gravity conditions are becoming available [28, 29] and when sufficient of these are available a detailed comparison of the models here with experiment can be made.

7. Summary

The close correspondence between the original chemical rate theory of Brailsford and Wynblatt [5] with the theories of Marqusee and Ross [12] and Enomoto *et al.* [15], all three of which have a very different basis, verifies the properties of the "effective medium" used in the chemical rate theory. The additional feature of the chemical rate theory, the matrix shell around the representative particle, is very plausible and imparts an additional flexibility to the theory which the present work demonstrates. Self-consistent versions of the theory have been developed using this aspect of the theory.

In this field, theoretical results are often not very accessible to those who wish to compare them with the results of experiment. Analytical expressions for particle size distributions as a function of volume fraction are provided herein together with tables of the parameters required for their evaluation. These also include values of the constant, γ, required for the evaluation of the rate constant for particle coarsening as a function of volume fraction. Computer programmes are also available on request to determine the distribution function and all the parameters involved in the expressions for any volume fraction.

The additional flexibility of the chemical rate theory which has been noted herein may allow it to produce relatively simple analytical expressions fitting the results of numerical simulation. These would be very efficient computationally when compared to the simulation itself and hence be useful to include in wider simulations. A possible example might be numerical simulation of the effect of particle coarsening on tertiary creep and remnant life prediction of components at temperatures and stresses at which creep can occur.

Appendix

Expressions for the parameters for calculation of the distribution functions.

Model 1—The Brailsford and Wynblatt [5] proposal $Y = y/\phi^{-1/3}$:

$$\left.\begin{aligned} b_1 &= 1 + \frac{3(1-\beta y_1)y_1^2}{\beta(y_c + y_1)^2(y_2 - y_1)} \\ b_2 &= \frac{3(1-\beta y_2)y_2^2}{\beta(y_c + y_2)^2(y_1 - y_2)} \\ c &= 1 + \frac{3(1-\beta y_c)y_c}{\beta(y_c + y_1)(y_c + y_2)} \\ a &= 2 + c + (b_1 - 1)y_c/y_1 + (b_2 - 1)y_c/y_2 \end{aligned}\right\} \quad \text{(A1)}$$

Model 2—$Y(y)$ represented by a quadratic, Equation 23, with P_3 having 3 real roots:

$$\left.\begin{aligned} b_1 &= 1 + \frac{3y_1^2\left(\lambda_0 - \lambda_1 y_1 + \lambda_2 y_1^2\right)}{\lambda_2(y_c + y_1)^2(y_2 - y_1)(y_3 - y_1)} \\ b_2 &= 1 + \frac{3y_2^2\left(\lambda_0 - \lambda_1 y_2 + \lambda_2 y_2^2\right)}{\lambda_2(y_c + y_2)^2(y_1 - y_2)(y_3 - y_2)} \\ b_3 &= 1 + \frac{3y_3^2\left(\lambda_0 - \lambda_1 y_3 + \lambda_2 y_3^2\right)}{\lambda_2(y_c + y_3)^2(y_1 - y_3)(y_2 - y_3)} \\ c &= \frac{3y_c\left(\lambda_0 + \lambda_1 y_c + \lambda_2 y_c^2\right)}{\lambda_2(y_c + y_1)(y_c + y_2)(y_c + y_3)} \\ a &= 2 + c + y_c[(b_1 - 1)/y_1 + (b_2 - 1)/y_2 \\ &\quad + (b_3 - 1)/y_3] \end{aligned}\right\} \quad \text{(A2)}$$

Model 2—$Y(y)$ represented by a quadratic, Equation 23, with P_3 having only 1 real root.

$$\left.\begin{aligned} b_1 &= 1 + \frac{3y_1^2\left(\lambda_0 - \lambda_1 y_1 + \lambda_2 y_1^2\right)}{\lambda_2(y_c + y_1)^2\left(y_1^2 - v' y_1 + w\right)} \\ c &= \frac{3y_c\left(\lambda_0 + \lambda_1 y_c + \lambda_2 y_c^2\right)}{\lambda_2(y_c + y_1)\left(y_c^2 + v' y_c + w'\right)} \end{aligned}\right\} \quad \text{(A3)}$$

We define

$$\left.\begin{aligned} K_1 &= (2 + b_1)/3 \\ K_2 &= (K_1 - 1)y_c/y_1 - c/3 \\ K_3 &= (1 - K_1)(2 - y_c v'/w')y_c \\ &\quad - c y_c(1 + y_1 v'/w')/3 \end{aligned}\right\} \quad \text{(A4)}$$

in terms of which

$$\left.\begin{aligned} a &= 2 + \frac{3\left[K_1 y_c^2/w' - K_2(2 - y_c/y_1) - K_3/y_1\right]}{1 + y_c v'/w' + y_c^2/w'} \\ b_2 &= 2 + (3K_1 - a)/2 \\ M &= \frac{(b_3 - 1)v' - w'(3K_2 + a - 2)}{\sqrt{w' - v'^2/4}} \end{aligned}\right\} \quad \text{(A5)}$$

Model 3—$Y(y)$ represented by a cubic, Equation 35, with P_4 having only 2 real roots:

$$\left.\begin{aligned} b_1 &= 1 + \frac{3y_1^2\left(\lambda_0 - \lambda_1 y_1 + \lambda_2 y_1^2 - \lambda_3 y_1^3\right)}{\lambda_3(y_c + y_1)^2(y_2 - y_1)\left(y_1^2 - v' y_1 + w'\right)} \\ b_2 &= 1 + \frac{3y_2^2\left(\lambda_0 - \lambda_1 y_2 + \lambda_2 y_2^2 - \lambda_3 y_2^3\right)}{\lambda_3(y_c + y_2)^2(y_1 - y_2)\left(y_2^2 - v' y_2 + w'\right)} \\ c &= \frac{3y_c\left(\lambda_0 + \lambda_1 y_c + \lambda_2 y_c^2 + \lambda_3 y_c^3\right)}{\lambda_3(y_c + y_1)(y_c + y_2)\left(y_c^2 + v' y_c + w'\right)} \end{aligned}\right\} \quad \text{(A6)}$$

We define

$$\left.\begin{aligned} K_1 &= (5 - b_1 - b_2)/3 \\ K_2 &= \tfrac{1}{3}[(b_2 - 1)y_c/y_2 - (b_1 - 1)y_c/y_1 - c] \\ K_3 &= -\tfrac{1}{3}\big[c y_c(y_1 + y_2 + y_1 y_2 v'/w') \\ &\quad + (b_1 - 1)\left(y_c^2 - 2y_c y_2 + y_c^2 y_2 v'/w'\right) \\ &\quad + (b_2 - 1)\left(y_c^2 - 2y_c y_1 + y_c^2 y_1\right)\big] \end{aligned}\right\} \quad \text{(A7)}$$

in terms of which

$$\left.\begin{aligned} a &= 2 + \frac{3\left[K_1 y_c^2/w' - K_2(2 - y_c/y_1 - y_c/y_2) - K_3/(y_1 y_2)\right]}{1 + y_c v'/w' + y_c^2/w'} \\ b_3 &= 2 + (3K_1 - a)/2 \\ M &= \frac{(b_3 - 1)v - w'(3K_2 + a - 2)}{\sqrt{w' - v'^2/4}} \end{aligned}\right\} \quad \text{(A8)}$$

References

1. W. OSTWALD, in "Analytische Chemie," 3rd ed. (Engelman, Leipzig, 1901) p. 23.
2. I. M. LIFSHITZT and V. V. SLYOZOV, *J. Phys. Chem. Solids* **19** (1961) 35.
3. C. WAGNER, *Z. Elektrochem.* **65** (1961) 581.
4. G. W. GREENWOOD, *Acta Metall.* **4** (1956) 243.
5. A. D. BRAILSFORD and P. WYNBLATT, *Acta Metall.* **27** (1979) 489.
6. A. J. ARDELL, *ibid.* **20** (1972) 61.
7. S. P. MARSH and M. E. GLICKSMAN, in "Modelling of Coarsening and Grain Growth," edited by S. P. Marsh and C. S. Pande (TMS, Warrendale, 1992).
8. J. H. YAO, K. R. ELDER, H. GUO and M. GRANT, *Physical Review B* **47** (1993) 14110.
9. M. K. CHEN and P. W. VOORHEES, *Modelling Simul. Mater. Sci. Eng.* **1** (1993) 591.
10. M. E. GLICKSMAN and P. W. VOORHEES, in "Phase Transformations in Solids," edited by T. Tsakalakos (North-Holland, Amsterdam, 1984) p. 451.
11. R. N. STEVENS and C. K. L. DAVIES, in "I Recontre transfrontalière Matèriaux Biphasiques," edited by A. Mateo, L. Lanes and M. Anglada (Barcelona, 1997) p. 21.
12. J. A. MARQUSEE and J. ROSS, *J. Chem. Phys.* **80** (1984) 536.
13. M. TOKUYAMA and K. KAWASAKI, *Physica* **123A** (1984) 386.
14. M. TOKUYAMA, K. KAWASAKI and Y. ENOMOTO, *ibid.* **134** (1986) 323.
15. Y. ENOMOTO, M. TOKUYAMA and K. KAWASAKI, *Acta Metall.* **34** (1986) 2119.
16. M. TOKUYAMA and Y. ENOMOTO, *Phys. Rev. E* **47** (1993) 1156.
17. M. MARDER, *Phys. Rev. A* **36** (1987) 858.
18. P. W. VOORHEES and M. E. GLICKSMAN, *Acta Metall.* **32** (1984) 2001
19. *Idem., ibid.* **32** (1984) 2013.
20. C. W. J. BEENAKKER, *Phys. Rev. A* **33** (1986) 4482.
21. D. FAN, L-Q CHEN, S. P. CHEN and P. W. VOORHEES, *Comp. Mater. Sci.* **9** (1998) 329.
22. N. AKAIWA and P. W. VOORHEES, *Phys. Rev. E* **49** (1994) 3860.
23. C. K. L. DAVIES, P. NASH and R. N. STEVENS, *Acta Metall.* **28** (1980) 179.
24. C. S. JAYANTH and P. NASH, *J. Mater. Sci.* **24** (1989) 3041.
25. P. W. VOORHEES, *J. Stat. Phys.* **38** (1985) 231.
26. *Idem., Annu. Rev. Mater. Sci.* **22** (1992) 192.
27. W. W. MULLINS and J. VIÑALS, *Acta Metall* **37** (1989) 991.
28. I. SEYHAN, L. RATKE, W. BENDER and P. W. VOORHEES, *Metall. Mat. Trans A* **27A** (1996) 2470.
29. J. ALKEMPER, V. A. SNYDER, N. AKAIWA and P. W. VOORHEES, *Phys. Rev. Letters* **82** (1999) 1725.

Received 17 January
and accepted 31 August 2001